

An adaptive numerical method for the Richards equation with root growth

Olga Wilderotter

Sonderforschungsbereich 256, Universität Bonn, Wegelerstrasse 6, D-53115 Bonn, Germany; e-mail: olga.wilderotter@de.ey.com

August 3, 2001

Abstract. An efficient new numerical method for simultaneously simulating soil water flow and plant root growth is presented. It allows the calculation of the water uptake of an entire root system while preserving the local impact of single roots. The approach is based on the adaptive finite-element method, which enables a flexible fine resolution along individual roots, which cannot be achieved by classical non-adaptive algorithms.

Keywords: root water uptake, root growth, adaptive finite-elements

1. Introduction

To model soil water uptake by roots, two alternative approaches have been developed in the past. The microscopic-scale approach studies water movement towards individual roots. The root system is considered as a set of connected axes, that grow and branch according to specific rules. In contrast, the macroscopic-scale approach regards the root system as an abstract object whose spatial distribution is described throughout the soil. Typical models in this category are root depths and root length density models. Both approaches have their respective merits, which have been intensely discussed in the literature. A detailed overview can be found in Smit et al. (2000).

A major difficulty of the microscopic approach is the inherent complexity of the root system. Nevertheless it is interesting to maintain the individuality of roots. Clothier and Green (1997) state that “entire root systems are dendritically complicated, and the fluxes of water to active roots range through all points of the compass. It is the local detail of this complex branching form that permits the plant to function effectively to extract sufficient water and chemicals against the capillary forces retaining them in the soil.”

In the last two decades several models of the root system architecture have been developed, e.g. (Rose, 1983; Pagés and Kervella, 1990; Berntson, 1992; Clausnitzer and Hopmans, 1994; Chikushi and Hirota, 1998). Clausnitzer and Hopmans (1994) developed an accomplished description of the root growth process. With respect to water

uptake these authors remark that “attempts have recently been made to numerically model water movement toward individual roots using the Richards equation (Bruckler et al., 1991; Lafolie et al., 1991). However, . . . the computational costs of simulating water movement on such a microscopic scale are still exceedingly high when considering complete root systems.”

The main contribution of the present paper is to show that the adaptive finite-element method is an efficient new computational technique to overcome these difficulties. It is ideally suited for problems involving two different scales. The essential idea is to use fine resolution along individual roots, while coarse resolution is sufficient in regions without roots. This allows coupling the root system architecture with the processes of water absorption and water flow in the soil. Our approach enables the upscaling of localized information on single roots into a comprehensive description of the root system as a whole.

In order to reach this goal, we combine a two-dimensional water flow model, which is based on the Richards equation, with a two-dimensional root growth model. A finite-element grid on the considered soil domain serves as the framework for the water flow model. The root system is simulated with the help of a cellular automaton and is coupled by the sink term with the Richards equation. Having merged both models, the numerical solution of the combined problem is then obtained by means of adaptive finite-elements.

The paper is organized as follows: Chapter 2 contains the mathematical equation describing soil water flow. Chapter 3 deals with modelling water extraction. This comprises the root system architecture model as well as the water uptake model. The mathematical algorithm for the adaptive finite-element resolution along individual roots is given in Chapter 4. Chapter 5 contains numerical examples illustrating the power of our approach. Chapter 6 sums up and discusses our results. In order to make the paper easier to read, we have consigned the mathematical details to two appendices. Moreover, all parameters and their units are listed in a separate appendix.

2. Soil water flow

The saturated/unsaturated water flow in a homogeneous porous media is described mathematically by the Richards equation

$$\partial_t \Theta(h) - \operatorname{div}(K(h) \nabla(h + z)) = F(h), \quad (2.1)$$

where $h[m]$ is the unknown pressure head, $\Theta[m^3 \cdot m^{-3}]$ is the volumetric soil water content, $K[m \cdot d^{-1}]$ is the soil hydraulic conductivity, $z[m]$

is the vertical space coordinate (positive upwards), $t[d]$ is the time and $F[d^{-1}]$ is the sink term to account for root uptake. The ∇ -operator is defined as the vector

$$\left(i \frac{\partial}{\partial x} + j \frac{\partial}{\partial y} + k \frac{\partial}{\partial z}\right)$$

with i, j and k denoting the positive unit vectors in x -, y -, and z -direction, respectively.

This equation was originally derived by L. A. Richards (Richards, 1931). Before solving the Richards equation one must supply parameters for the functions $\Theta(h)$ and $K(h)$. For parametrizing the relationship between the water content and the pressure we use the Van Genuchten approach (Van Genuchten, 1980)

$$\Theta(h) = \Theta_r + (\Theta_s - \Theta_r) \left(\frac{1}{1 + (-ah)^n} \right)^m \quad (2.2)$$

with $m = 1 - 1/n$. Here Θ_r and Θ_s denote the residual and the saturated volumetric water content, respectively. The parameters $a > 0, n > 1$ have to be specified for each soil type. For parametrizing the relationship between the hydraulic conductivity and the pressure we use the Mualem model (Mualem, 1976)

$$K(S) = K_s S^{1/2} (1 - (1 - S^{1/m})^m)^2, \quad (2.3)$$

where $K_s[m \cdot d^{-1}]$ is the saturated conductivity and $S[m^3 \cdot m^{-3}]$ is the normalized volumetric water content defined as

$$S = \frac{\Theta - \Theta_r}{\Theta_s - \Theta_r}.$$

The numerical solution of (2.1) is based on the Jäger-Kačur scheme, which is a new, very efficient algorithm for solving degenerate, parabolic differential equations (Jäger and Kačur, 1995). Since the algorithm of the Jäger-Kačur is mathematically intricate, we have consigned the details to Appendix 1.

3. Modelling of water extraction

3.1. THE ROOTSYSTEM AND ITS GROWTH

As said in the introduction, there are two main categories of models describing root growth, viz. macroscopic root depth and root length density models and microscopic models of the root system architecture.

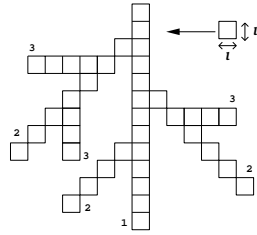


Figure 1. Cellular automaton.

In the present paper we simulate root growth with the help of a cellular automaton. This approach belongs to the second category of models.

Geometrically, the root system is a set of cells, the length of which is increased by elongation and branching of its members. A hierarchy of root members may be defined among the axes, according to their order. By Cannon's classification (1949) we shall call the axes directly connected to the shoot system order 1 axes, the axes extending from the axes of order 1 order 2 axes and so on (Figure 1). This distinction among root axes is not purely formal, because axes of different order also differ in their morphology.

The extension of the root system is simulated in discrete time steps, by applying three formalised developmental processes to the existing root system at each time step. These are root emission (i.e. generation of new root axes from the shoot system), growth (i.e. elongation of existing axes), and branching (i.e. development of new lateral axes). We use different time intervals for the root development simulation and for the water flow model. The time steps for the root development model are of constant length, while the time steps for the soil water flow model are automatically adjusted as will be described below. The rules for the root system extension are based primarily on Pagés and Kervella (1990). Growth is, however, also a function of the local conditions in our model. To define the growth direction and elongation rate, we use the data on local water content as calculated according to the water flow model.

Emission In the case of a primary root system only one root axis of order 1 is emitted. At the beginning we must specify the starting point of this axis and its growth direction. To achieve this, we choose one cell from our cellular automaton, which is located directly under the soil surface and assume that this cell will start growing directly downwards (Figure 2). The growth and branching of this cell will give rise to lateral roots of order 2 and 3.

Growth The growth of all existing axes always starts at the tip of the root. We must specify the growth direction and length of each axis for each growth time step. We assume that for each branch there are 5

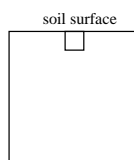


Figure 2. Emission.

possible directions of growth. These directions are shown in Figure 3. The cell marked with the letter "s" describes the tip of the root. The

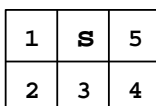


Figure 3. Possible growth directions.

model assumes that one growth direction is more probable than the others. For an axis of order 1 this is vertical, and for axes of order two and order three it is at an angle of 45 degrees to the mother axis (Figure 4). Our model allows, however, that axes may deviate from

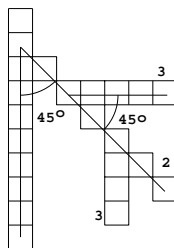


Figure 4. More propable growth directions.

their preferred direction towards a direction of higher water content.

For these reasons the growth direction is fixed at each point of time t_w , when the root grows, as in the following: Cell "s" represents the tip of the branch, and "r" is the next cell in the preferred growth direction. Let "threshold" be a given value in the interval $(0, 1)$ and "rnd_num*b_i*", $i \in [1, 5]$, a sequence of random numbers between 0 and 1. First we set the growth direction equal to the preferred direction "r". Then we check for the elements $i \in [1, 5]$, $i \neq r$ the following condition:

$$threshold(\Theta(i) - \Theta(s)) rnd_numb_i > (\Theta(r) - \Theta(s)) rnd_numb_r.$$

For a small "threshold" the moisture content in a direction other than the preferred one must be very high, in order to divert the root growth in this direction. Conversely a high "threshold" supports growth towards moisture. Thus we consider only water content as the driving force for root growth.

Other aspects which determine the trajectories of roots have been simulated by Clausnitzer and Hopmans (1994). In their description they include the direction of the root tip in the previous time phase, a random deviation representing the space-exploring behaviour of the root tip, geotropism along an angle to the horizontal plane and the negative soil strength gradient.

Having chosen the growth direction, we must now determine the elongation rate $er[m \cdot d^{-1}]$. In general this rate is influenced by the species of the plant, water content, temperature, nutrient content and the order of the axes. In our model we will take two factors that influence the elongation rate into consideration: the water content and the order of the root. In order to find the elongation rate for a certain branch, we calculate the pressure head value in the cell, that lies next to the tip of the branch in the growth direction. Depending on this result we set the variable "er". Let $er = k \cdot l$, where $l[m]$ denotes the cell length. The function $k[d^{-1}]$ measures the number of cells, for which the corresponding branch will be prolonged in the present time step. This function is piecewise constant and depends as well on the pressure head as on the root order. A possible choice of k for the root order one is shown in Figure 5. The pressure values h_i , $i = 1, 2, 3, 4, 5$ as well as the factors k_i , $i = 1, 2, 3, 4, 5$ must be set by the user. The elongation

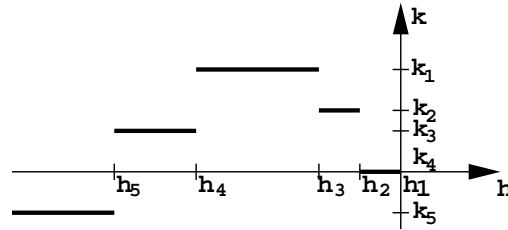


Figure 5. Elongation rate.

rate decreases with the order of the branches. For the roots of order two we choose the values for the elongation rate identical to the root order 1. The values for the third hierarchical degree are obtained by halving the k_i values of order 2.

Root branching Studies of the root distribution along the mother axis show that this distribution is not random (Riopell, 1969; Mallory et al., 1970; Charlton, 1983). The youngest side roots are separated from the tip of the mother axis by a relatively extensive apical non-branching zone. In order to model these phenomena, two variables are defined (Lungley, 1973; Pagés and Aries, 1988):

- the length of the apical non-branching zone (LAZ[m]);
- the inter-branch distance along the axis (IBD[m]).

For each root growth time step and each axis the possibility of root

branching is tested. If the distance between the tip of a branch and the last lateral branch along that axis is larger than the sum of the two variables LAZ and IBD, then a new root is initiated at a distance IBD from the preceding side root, as exemplified in Figure 6. Here the upper left side roots and the right side roots already exist. We observe, how a new side branch of order two is formed on the left at the IBD distance below the right second order side root. Both variables LAZ and IBD depend on the order of a branch and are quantified during the computer simulation. Finally we assume that the formation of lateral roots is equally distributed to the left and right side of the mother axis.

To model the acropetal branching, other authors (Diggle, 1988; Clausnitzer and Hopmans, 1994) also consider the duration of apical non-branching, i. e. new branches can only appear on parts of the mother root having reached a given age.

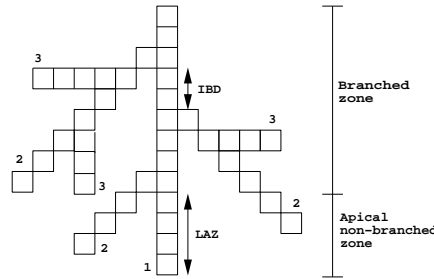


Figure 6. Formation of a new lateral root.

3.2. MODEL FOR THE SINK

The term F in the Richards equation is defined equal to the volume of water extracted from a unit volume of soil per unit time. There are different approaches to describe this term (Molz, 1981; Smit et al., 2000). The process of water extraction by roots involves both plant and soil factors. Our approach is flexible enough to deal with both phenomena. For this purpose we consider the soil and root resistance as a system of two resistors in series. Using an analogy of Ohm's law we conclude that the flux density $Q[m^3 \cdot m^{-2} \cdot s^{-1}]$ of water entering the root is given by

$$Q = \frac{h - h_w}{R_s + R_r}. \quad (3.4)$$

Here $h_w[m]$ is the pressure head in the root, $R_s[d]$ is the soil resistance and $R_r[d]$ is the root resistance. Formula (3.4) was already formulated by Gardner and Ehlig (1962). Since then it has been used and refined by many other authors, for example (Hillel et al., 1975; Radcliffe et al., 1986; Biondini, 2001).

The soil resistance can be taken as directly proportional to the flow path length and inversely to the hydraulic conductivity. The root resistance has been investigated by several researchers (Landsberg and Fowkes, 1978; Frensch and Steudle, 1989; Alm et al., 1992; Aura, 1996; Doussan et al., 1998). In wet soil water root uptake is primarily determined by the root resistance. As the soil dries, the influence of the soil resistance increases, and root shrinkage may reduce the liquid-phase continuity between a root and the surrounding soil. This variable contact resistance was first quantitatively evaluated by Herkelrath et al. (1977). These authors multiplied the uptake rate by a factor Θ/Θ_s , which accounts for the soil-root contact resistance. The effects of limited root-soil contact have been further studied by Faiz and Weatherley (1978), Hansen et al. (1991), Bouten (1992).

More details on the types of resistance to water movement in the soil-root system can be found in the monographs of Kramer and Boyer (1995), Smit et al. (2000), Lösch (2001) as well as in the recent reviews by Hopmans and Bristow (2002), Mmolawa and Or (2000).

The above discussion shows that various different effects influence the way roots extract water. A main advantage of our finite-element algorithm is that different kinds of uptake functions can be implemented flexibly.

So far we have dealt with the flux density Q of water entering the root. In order to obtain the sink term F , we must next calculate the volume of water extracted by a single cell of our automaton. Assuming each cell to be a cube with edge length l , which absorbs water through its 4 lateral sides, we conclude that the water volume extracted per unit time by one cell of our automaton is equal to $Q \cdot 4l^2$. Division of this expression by the cube volume l^3 yields the following form of the sink term in the Richards equation:

$$F(x, y, t, h) = \frac{h - h_w}{R_s + R_r} l^{-1} \rho(x, y, t).$$

Here ρ is a dimensionless indicator function, which is equal to 4 inside the cells of the automaton and 0 otherwise.

A disadvantage of the cellular automaton considered is that the cell distribution is not realistic at locations in diagonal branches, where cells meet only in one corner. A possible way to cope with this problem is the addition of halfcells, which are located above and beneath such cells, to our rootsystem. Thus one replaces the root system from Figure 1 by the root system shown in Figure 7.

A second way to handle cells, which meet only in one corner, is the smoothing of F by convolution. Instead of F the function $G_\sigma * F$ is

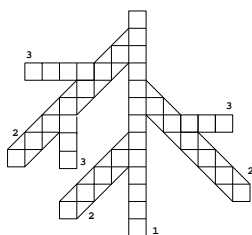


Figure 7. Smoothing of the root system

used, where G_σ denotes the Gauß-kernel:

$$G_\sigma(x, y) = \frac{1}{(2\sqrt{\pi\sigma})^2} e^{-\frac{(x^2+y^2)}{4\sigma}}.$$

Numerically the size of the actual discrete time step is a good choice for the smoothing parameter σ .

3.3. IMPLEMENTING THE CELLULAR AUTOMATON ON THE COMPUTER

First of all we fix the root thickness l and divide the given rectangular domain Ω in quadrates of length l . The cells are numbered - starting from the top - from left to right and summarized in an array (Figure 8). This field forms our cellular automaton. It consists of structures of

1	2	3	4	5	6	7	...		

Figure 8. Initiating of cellular automaton

type CELL. Each structure contains the following cell information:

- affiliation to the root system;
- cell location: inside or on the boundary of the domain Ω .

For the description of the whole root system, a structure ROOTSYSTEM is built. It contains the total number of already existing branches as well as pointers to the cellular automaton and the main axis of order 1. The information about each individual branch is stored in the structure BRANCH. This structure contains information about:

- order of the branch;
- time of origination of the branch;
- branch length expressed by the number of cells;

- branch-free length;
- cell number of the original cell;
- cell number of the tip;
- preferred growth direction;
- array with the numbers of all cells pertaining to this branch;
- pointer to the next branch of equal order with the same mother axis;
- pointer to the first lateral root of the current branch.

Using this storage structure one can easily traverse all branches.

Initiating the cellular automaton consists of marking the cells already originated in the main root of order 1. Moreover, the total number of branches must be set to 1, since at the beginning only one single root exists. Next, information about this initial root is written into the storage space provided for this structure.

After initiating the variables, the root growth process has to be implemented. It is schematically described by the following pseudo code. For each growth time step, the function `RootGrowth` is started:

```

RootGrowth{
    branch = rootsystem → macrobranch;
    TreatBranch;
    branch = branch → firstchild;
    while(branch){
        TreatBranch;
        child = branch → firstchild;
        while(child){
            TreatBranch;
            child = child → next;
        }
        branch = branch → next;
    }
    TreatBranch{
        Growth;
        Branching;
    }
    Growth{
        choose growthdirection;
    }

```

```

    calculate elongationrate;
    extend branch in growthdirection by elongationrate;
}
Branching{
    if(branch → nonbranchinglength > LAZ + IBD)
        initial new child;
}

```

4. Adaptivity

We use adaptivity in order to compute the numerical solution efficiently as well as to cope with the complexity of the root system. Our aim is the computation of an approximate pressure head distribution, such that the error e (i. e. the difference between the exact and the approximate solution) lies under a given tolerance.

For this purpose we have to discretize our problem with respect to time and space. Time is discretized by means of the Jäger-Kačur scheme (see Appendix 1). Space is discretized by using a finite-element triangulation for the soil domain Ω under consideration. All functions on Ω are approximated by piecewise linear finite-elements. The decisive trick lies in the fact that the underlying triangulation is not static, but can be dynamically adapted. This means that some triangles will be refined while others will be coarsened depending on the properties of the approximate solution actually calculated. Intuitively speaking, the mesh must be refined, where the solution shows steep gradients and oscillations. Conversely, the mesh can be coarsened in regions, where the solution is smooth.

In order to formulate our adaptive strategy precisely, we introduce three error estimators:

- (i) the initial error estimator E_0 copes with that part of the error, which stems from approximating the initial pressure head distribution at time point t^0 by piecewise linear finite-elements.
- (ii) the time error estimator E_τ^i yields an upper bound for the difference between the numerical solution evaluated at time point t^i and the numerical solution evaluated at time point t^{i-1} .
- (iii) the grid error estimator E_h^i gives an upper threshold for the spatial discretization error of the finite-element approximation at time point t^i .

We omit the technical details of how to construct E_0 , E_τ^i and E_h^i . A comprehensive description is given in Wilderotter (2001). Here we only summarize the following important properties:

- (i) The error estimators can be explicitly computed since they only depend on the data of the problem and on the numerical solution already calculated, but not on the unknown analytical solution.
- (ii) E_0 , E_h are compounded from local quantities $E_0(T)$ and $E_h^i(T)$, which can be computed on each triangle T of our domain Ω :

$$E_0 = \sum_{T \in \mathcal{T}^0} E_0(T), \quad E_h^i = \sum_{T \in \mathcal{T}^i} E_h^i(T)$$

Here \mathcal{T}^0 and \mathcal{T}^i represent the triangulations at the point t^0 and t^i , respectively.

- (iii) The computational costs for calculating E_0 , E_τ^i and E_h^i are low.

Geometrically, E_0 is responsible for the spatial adaptive refinement of Ω at the initial time t^0 , while E_h^i does the same job for time points t^i following t^0 . E_τ^i controls the size of the time step. This size is automatically adjusted to optimize overall simulation time and convergence behavior within each time step.

We recall that our final aim is to approximately compute the pressure head distribution with a guaranteed accuracy TOL. With this in mind, our adaptive method now reads as follows:

Algorithm

Step I. Initially, the domain Ω is refined until $E_0 \leq \text{TOL}$.

Step II. In the second step we iterate the SERC-algorithm. SERC stands for

Solve - Estimate - Refine - Coarsen.

The i -th iteration looks like the following:

- 1 At the time point t^i we compute the numerical pressure head distribution in the form of a piecewise linear finite-element approximation on the actual triangulation. In order to obtain this finite-element approximation, we must solve a system of nonlinear equations.
- 2 We calculate E_τ^i and check whether $E_\tau^i > \text{TOL}$. If this is the case, we reduce the time step from t^{i-1} to t^i and choose a smaller value for t^i . Then we go to (1).

- 3 We calculate $E_h^i(T)$ for every triangle T of our triangulation. We refine those triangles T where $E_h^i(T)$ is not small enough, while we coarsen triangles T where $E_h^i(T)$ is too small.
- 4 When the mesh has been changed, we go to (1) and solve the nonlinear equation system once more, this time, however, with the modified triangulation. In this way we obtain a new improved finite-element approximation for the time point t^i .
- 5 Finally, we choose the next time point t^{i+1} depending on the size of E_τ^i .

The above description is only a rough sketch of the algorithm. The complete implementation is mathematically much more intricate and summarized in Appendix 2.

5. Numerical example

Now we demonstrate the power of our method by an example. We consider root water uptake in a quadrate of soil with two meter side length, whose upper boundary coincides with the soil surface: $\Omega = (0, 2)^2$ (Figure 9). The total simulation time T is 75 days. The ground-water level

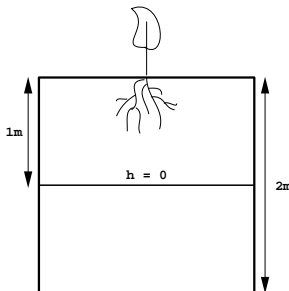


Figure 9. Cross-section of soil.

is initially located at a depth of one meter under the soil surface. The initial pressure is in hydrostatic equilibrium with this surface. The lower and the vertical boundaries are assumed to be impermeable. On the upper boundary we assume a non-flow condition. The soil parameters in (2.2), (2.3) are set as follows:

$$\Theta_r = 0.0, \quad a = 0.15, \quad K_s = 0.001, \quad \Theta_s = 0.4, \quad n = 1.9.$$

The parameters of the root growth model are quantified in Table I. Finally the soil resistance is given by $R_s = l/K(\Theta)$. The root resistance

Table I. Parameters of the root growth model

$l[m]$	2^{-7}	root thickness
$\tau_w[d]$	1.0	time step for root growth
δ	1.7	factor to adjust the time step
threshold	0.07	value for determining the growth direction
LAZ[m]	32l	non-branching zone for branches of order 1
	16l	non-branching zone for branches of order 2
IBD[m]	16l	distance between two branches of order 2
	10l	distance between two branches of order 3
$h_w[m]$	-50.0	pressure in the root
$h_1[m]$	0.0	
$h_2[m]$	-0.05	
$h_3[m]$	-0.2	pressure values to determine the elongation rate
$h_4[m]$	-10.0	
$h_5[m]$	-20.0	
$k_1[d^{-1}]$	4	
$k_2[d^{-1}]$	2	
$k_3[d^{-1}]$	2	factors to determine the elongation rate
$k_4[d^{-1}]$	0	
$k_5[d^{-1}]$	-2	

is the reciprocal of the root hydraulic conductivity and was calculated from the values found in Doussan et al. (1998), see also Frensch and Steudle (1989): $R_r = 5.2 \cdot 10^3[d]$.

Figures 10-15 show the pressure head distribution and the corresponding grids for the time sequence $t \in \{10, 25, 40, 55, 65, 75\}$. As expected, we observe a strong refinement along the roots. The black line in the middle of the square shows the ground-water level. When the roots begin to grow, they absorb water from the surrounding soil. The soil becomes dry from water uptake and the ground-water level falls slowly.

6. Conclusions

A new computational approach for simulating water uptake by plant roots has been developed. The basic idea is as follows: Use fine resolution near the roots, where interesting local effects are to be expected. In contrast, use coarse resolution in soil regions farther from the roots, where the solution is predicted to be smooth. Since the location and distribution of the roots changes continuously during the growth process,

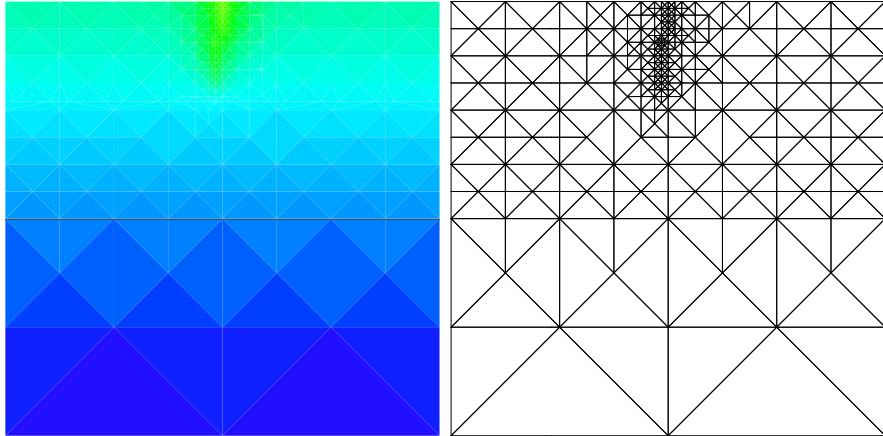


Figure 10. Pressure distribution and adaptive refined grids for $t = 10.0$

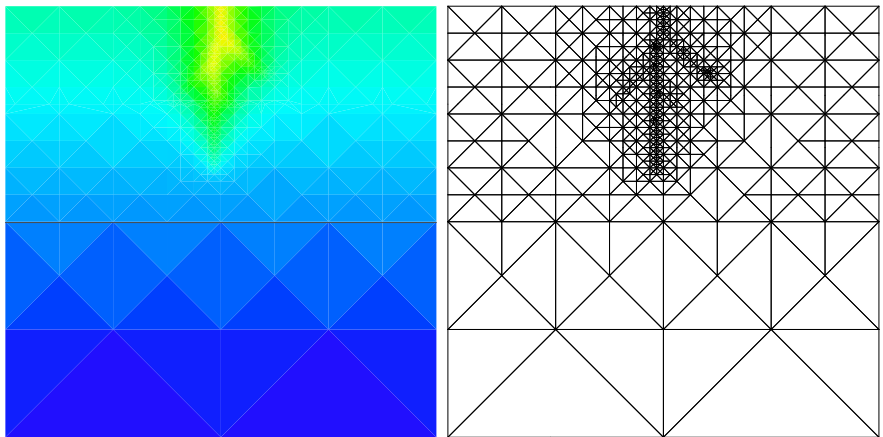


Figure 11. Pressure distribution and adaptive refined grids for $t = 25.0$

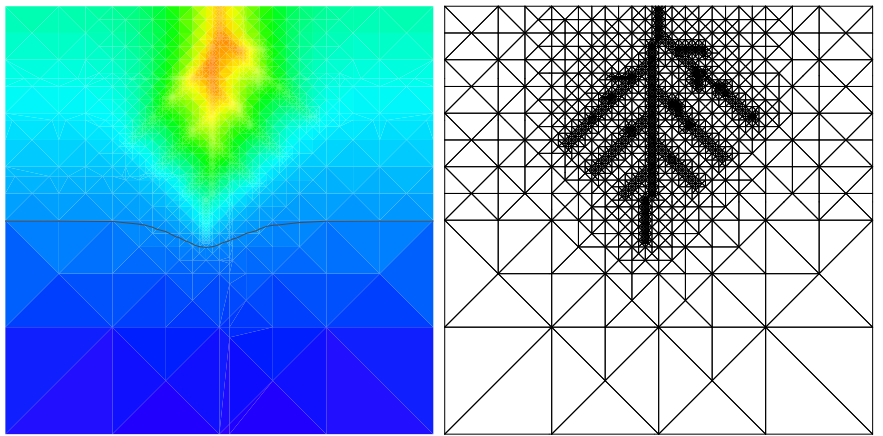


Figure 12. Pressure distribution and adaptive refined grids for $t = 40.0$

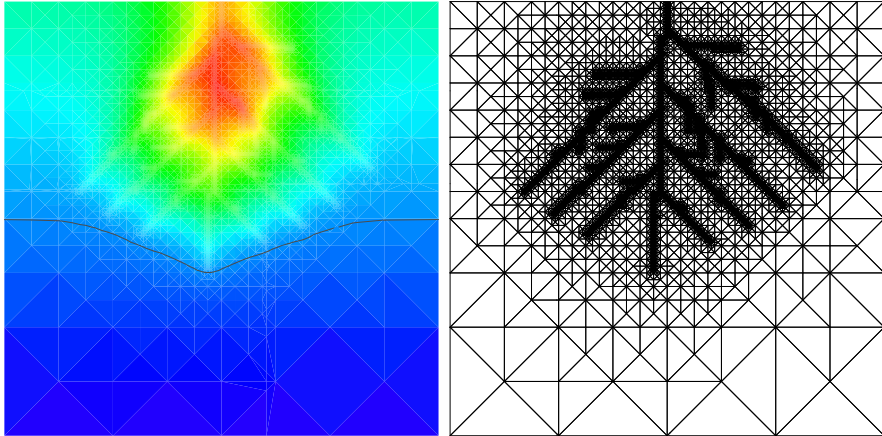


Figure 13. Pressure distribution and adaptive refined grids for $t = 55.0$

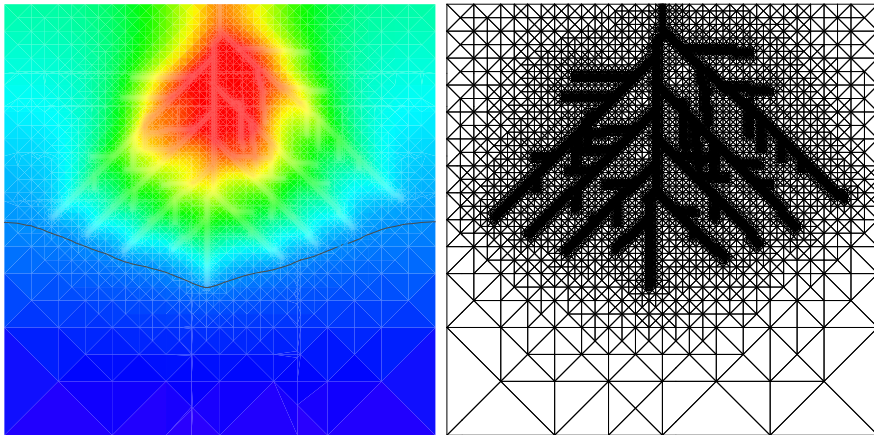


Figure 14. Pressure distribution and adaptive refined grids for $t = 65.0$

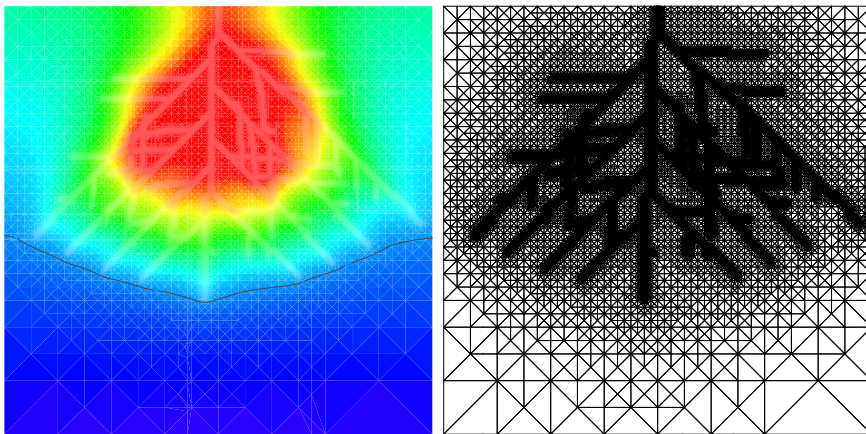


Figure 15. Pressure distribution and adaptive refined grids for $t = 75.0$

it is of decisive numerical importance, that the discretization mesh is adapted dynamically. This allows calculations and simulations of root water uptake scenarios, which are not feasible when working with static fixed meshes.

A main advantage of our approach is its flexibility. Various microscopic root growth models can be included. In the present paper we used a relatively simple prototype, in order to make clear the fundamental ideas of two scale problems. We emphasize, however, that our approach can be definitely extended to the architecture of more complex root system models. Moreover, the sink term can be chosen in such a way that the root resistance as well as the soil resistance are both taken into consideration. Different models for quantifying the influence of the root and soil resistance on water extraction can be implemented and tested.

The adaptive finite-element method can help substantially to understand the link between rootzone form and function by performing virtual experiments on the computer. We agree with Pagés et al. (2000), who state, “that acquisition of resources within the soil environment is a complex process . . . Thus, models should mix different formalisms for representing at the same time physical processes (e.g. Darcy’s law) and biological ones (e.g. root growth). These models should also succeed in the integration of several organisation levels.”

In the present paper we successfully combined a model for water flow based on Richards equation with a root growth model. Moreover, we showed that the adaptive finite-element method is an important contribution for computationally upscaling from the individual root level to the level of a complete root system.

Appendix

A. The Jäger-Kačur scheme

In order to solve the Richards equation (2.1) numerically, we convert it by means of the Kirchoff transformation $u = T(h) = \int_0^h K(s)ds$ in the following form

$$\partial_t b(u) - \operatorname{div}(\nabla u + K(b(u))e_z) = F(b(u)), \quad (\text{A.5})$$

where e_z is the unit vector in upward z -direction and $b(u) = \Theta(h)$. Numerically, we will solve the Richards equation in the form (A.5). In this way we will obtain the distribution of the water content $\Theta(h) =$

$b(u)$ as well as u . The pressure head h can then be computed from u by inversion of the Kirchoff transformation: $h = T^{-1}(u)$.

The numerical solution of equation (A.5) is computed iteratively with help of the Jäger-Kačur scheme.

Let τ^i be the i -th time step and $t^i = \sum_{l=1}^i \tau^l$. Given the numerical solution U^{i-1} at time point t^{i-1} , we want to calculate the solution U^i at time point t^i . For this purpose we look for a parameter μ^i and a function θ^i such that

$$\mu^i \theta^i - \tau^i \Delta \theta^i = \mu^i U^{i-1} + \tau^i \nabla \cdot K(b(U^{i-1})) - \tau^i F(b(U^{i-1})), \quad (\text{A.6})$$

where the relaxation parameter μ^i must satisfy the following convergence condition:

$$\frac{\epsilon}{2} \leq \mu^i \leq \frac{b_\epsilon(U^{i-1} + \lambda(\theta^i - U^{i-1})) - b_\epsilon(U^{i-1})}{\theta^i - U^{i-1}} \quad (\text{A.7})$$

with $0 < \epsilon = o(1)$ and with the parameter $\lambda \in (0, 1)$ close to 1. Having determined μ^i and θ^i , the solution U^i at the new time point t^i is now obtained by algebraic correction:

$$b_\epsilon(U^i) = b_\epsilon(U^{i-1}) + \mu^i(\theta^i - U^{i-1}).$$

Here b_ϵ denotes the regularization of b defined as

$$b_\epsilon(s) = \begin{cases} b(s) + \epsilon s & \text{for } s > 0 \\ b(s) & \text{for } s \leq 0 \end{cases}$$

The scheme (A.6), (A.7) is implicit with respect to μ^i and θ^i and must therefore be solved by some special kind of fixed point iterations, the so called **inner iterations**.

B. The adaptive refinement algorithm

For the space discretization we use linear finite-elements. By \mathcal{T}^i we denote a sequence of subsequently refined/coarsened triangulations of Ω into triangles T with usual regularity properties as in Ciarlet (1978). $\mathcal{N}_{\mathcal{T}^i}$ is the number of triangles in \mathcal{T}^i . For refinement we use the bisection (Bänsch, 1991). Coarsening was described in detail by Nochetto et al. (1997). In order to calculate a finite-element approximation U^i on \mathcal{T}^i with a guaranteed accuracy TOL, we proceed as follows:

Let $\Gamma_0, \Gamma_\tau, \Gamma_h > 0$ be given refinement parameters and let $\gamma_\tau, \gamma_h > 0$ be given coarsening parameters with

$$\Gamma_0 + \Gamma_\tau + \Gamma_h \leq 1, \quad \gamma_\tau < \Gamma_\tau, \quad \gamma_h < \Gamma_h.$$

Step I. In the first step a given macro-triangulation \mathcal{T}^0 is made finer according to the data. We refine all $T \in \mathcal{T}^0$ with

$$E_0(T) > \frac{\Gamma_0^2 \text{TOL}^2}{\mathcal{N}_{\mathcal{T}^0}}$$

and prolongate U^0 onto the new grid by interpolation. We continue until

$$E_0 \leq \Gamma_0^2 \text{TOL}^2.$$

Step II. In the second step, we iterate the SERC-algorithm. SERC stands for

Solve - Estimate - Refine - Coarsen.

The i -th iteration looks like follows:

- 1 Set $t^i = t^{i-1} + \tau^i$ and solve the system of equations.
- 2 In order to select the time step τ^i , the algorithm checks whether

$$\sum_{T \in \mathcal{T}^i} E_\tau^i(T) > \frac{\Gamma_\tau^2 \text{TOL}^2}{4}.$$

If this is the case, τ^i is reduced and we go to (1).

- 3 In order to adapt the grid, we check whether

$$E_h^i(T) > \frac{\Gamma_h^2 \text{TOL}^2}{4\mathcal{N}_{\mathcal{T}^i}}, \quad E_h^i(T) < \frac{\gamma_h^2 \text{TOL}^2}{4\mathcal{N}_{\mathcal{T}^i}}.$$

In the first case we refine T , whereas in the second one we coarsen T .

- 4 When the mesh has been changed, we recalculate and compute U^i .
- 5 We test the time step size once more. If

$$\sum_{T \in \mathcal{T}^i} E_\tau^i(T) > \frac{\Gamma_\tau^2 \text{TOL}^2}{4},$$

we reduce τ^i and continue with (1).

- 6 The space discretization is tested once more. If

$$\sum_{T \in \mathcal{T}^i} E_h^i(T) > \frac{\Gamma_h^2 \text{TOL}^2}{4},$$

then we go to (3). Otherwise we accept U^i , \mathcal{T}^i and τ^i .

Table II. Parameter set used in the paper

Symbol	Definition	Units
Basic variables		
t	time	d
z	depth	m
Soil parameters		
Θ	volumetric soil water content	$m^3 \cdot m^{-3}$
h	pressure head	m
K	hydraulic conductivity	$m \cdot d^{-1}$
F	sink term to account for root uptake	d^{-1}
Plant parameters		
l	root thickness	m
LAZ	length of non-branching zone	m
IBD	distance between two branches of the same order	m
h_w	pressure in the root	m
er	elongation rate	$m \cdot d^{-1}$
$h_i, i = 1, \dots, 5$	pressure values for elongation rate	m
$k_i, i = 1, \dots, 5$	factors for elongation rate	d^{-1}

7 We set $\mathcal{T}^{i+1} = \mathcal{T}^i$, $\tau^{i+1} = \tau^i$. If

$$\sum_{T \in \mathcal{T}^i} E_\tau^i(T) < \frac{\gamma_\tau^2 \text{TOL}^2}{4},$$

then we enlarge τ^{i+1} .

8 If t^{i+1} is less than the simulation endpoint \mathbb{T} , we set $i = i + 1$ and continue with (1).

C. List of symbols used

In Table II we describe the main variables and parameters used in our paper.

Acknowledgements

The author is grateful to M. Rumpf for inspiring discussions.

References

- Alm, D. M., J. Cavelier, and P. S. Nobel: 1992, 'A finite element model of radial and axial conductivities for individual roots: Development and validation for two desert succulents.'. *Annals of Botany* **69**, 87–92.
- Aura, E.: 1996, 'Modelling non-uniform soil water uptake by a single plant root.'. *Plant and Soil* **186**, 237–243.
- Bänsch, E.: 1991, 'Local mesh refinement in 2 and 3 dimensions.'. *IMPACT Comput. Sci. Eng.* **3**, 181–191.
- Berntson, G. M.: 1992, 'A computer program for characterizing root system branching patterns.'. *Plant and Soil* **140**, 145–149.
- Biondini, M.: 2001, 'A three-dimensional spatial model for plant competition in an heterogeneous soil environment.'. *Ecol. Modell.* **142**, 189–225.
- Bouten, W.: 1992, 'Monitoring and modelling forest hydrological processes in support of acidification research.'. Ph.D. thesis, University of Amsterdam, Amsterdam.
- Bruckler, L., F. Lafolie, and F. Tardieu: 1991, 'Modeling root water potential and soil-root water transport. II. Field comparisons.'. *Soil. Sci. Soc. Am. J.* **55**, 1213–1220.
- Cannon, W. A.: 1949, 'A tentative classification of root system.'. *Ecology.* **30**, 542–548.
- Charlton, W. A.: 1983, 'Patterns of distribution of lateral root primordia.'. *Ann. Bot.* **51**, 417–427.
- Chikushi, J. and O. Hirota: 1998, 'Simulation of root development based on the dielectric breakdown model.'. *Hydr. Sciences* **43**, 549–560.
- Ciarlet, P. G.: 1978, *The finite element method for elliptic problems*. Amsterdam: North-Holland.
- Clausnitzer, V. and J. W. Hopmans: 1994, 'Simultaneous modeling of transient three-dimensional root growth and soil water flow.'. *Plant and Soil* **164**, 299–314.
- Clothier, B. E. and S. R. Green: 1997, 'Roots: the big movers of water and chemical in soil.'. *Soil Science* **162**, 534–543.
- Diggle, A. J.: 1988, 'ROOTMAP – a model in three-dimensional coordinates of the growth and structure of fibrous root systems.'. *Plant and Soil* **105**, 169–178.
- Doussan, C., L. Pagés, and G. Vercambre: 1998, 'Modelling of the hydraulic architecture of root systems: An integrated approach to water absorption. I. Model description.'. *Annals of Botany* **81**, 213–223.
- Faiz, S. M. A. and P. E. Weatherley: 1978, 'Further investigations into the location and the magnitude of the hydraulic resistances in the soil-plant system.'. *New Phytol.* **81**, 19–28.
- Frensch, J. and E. Steudle: 1989, 'Axial and radial hydraulic resistance to roots of maize (*Zea mays* L.)'. *Plant Physiol.* **91**, 719–726.
- Gardner, W. R. and C. F. Ehlig: 1962, 'Some observations on water movement to plant roots.'. *Agron. J.* **54**, 453–456.
- Hansen, S., H. E. Jensen, N. E. Nielsen, and H. Svendsen: 1991, 'Simulation of nitrogen dynamics and biomass production in winter wheat using the Danish simulation model DAISY.'. *Fert Res* **27**, 245–261.
- Herkelrath, W. M., E. E. Miller, and W. R. Gardner: 1977, 'Water uptake by plants: II. The root contact model.'. *Soil. Sci. Soc. Am. J.* **41**, 1039–1043.
- Hillel, D., C. G. E. M. van Beek, and H. Talpaz: 1975, 'A microscopic-scale model of soil water uptake and salt movement to plant roots.'. *Soil Science* **120**, 385–399.

- Hopmans, J. W. and K. L. Bristow: 2002, ‘Current capabilities and future needs of root water and nutrient uptake modeling.’. *Advances in Agronomy* **77**, 103–183.
- Jäger, W. and J. Kačur: 1995, ‘Solution of doubly nonlinear and degenerate parabolic problems by relaxation schemes’. *RAIRO, Modelisation Math. Anal. Numer.* **29**, 605–627.
- Kramer, P. J. and J. S. Boyer: 1995, *Water Relations of Plants and Soils*. San Diego: Academic Press.
- Lafolie, F., L. Bruckler, and F. Tardieu: 1991, ‘Modeling root water potential and soil–root water transport. I. Model presentation.’. *Soil. Sci. Soc. Am. J.* **55**, 1203–1212.
- Landsberg, J. J. and N. D. Fowkes: 1978, ‘Water movement through plants.’. *Annals of Botany* **42**, 493–508.
- Lösch, R.: 2001, *Wasserhaushalt der Pflanzen*. Wiebelsheim: Quelle & Meyer Verlag.
- Lungley, D. R.: 1973, ‘The growth of root systems – a numerical computer simulation model.’. *Plant and Soil* **38**, 145–159.
- Mallory, T. E., S. H. Chiang, E. G. Cutter, and E. J. Gifford: 1970, ‘Sequence and pattern of lateral root formation in five selected species.’. *Am. J. Bot.* **57**, 800–809.
- Mmolawa, K. and D. Or: 2000, ‘Root zone solute dynamics under drip irrigation: A review.’. *Plant and Soil* **222**, 163–190.
- Molz, F. J.: 1981, ‘Models of water transport in the soil–plant system: a review.’. *Wat. Res. Res.* **17**, 1245–1260.
- Mualem, Y.: 1976, ‘A new model for predicting the hydraulic conductivity of unsaturated porous media.’. *Water Resour. Res.* **12**, 513–522.
- Nochetto, R. H., A. Schmidt, and C. Verdi: 1997, ‘Adapting meshes and time-steps for phase change problems’. *Quaderno, Milano* **12**.
- Pagés, L. and F. Aries: 1988, ‘SARAH: modèle de simulation de la croissance, du développement et de l’architecture des systèmes racinaires.’. *Agronomie* **8**, 889–896.
- Pagés, L., C. Doussan, and G. Vercambre: 2000, ‘An introduction on below–ground environment and resource acquisition, with special reference on trees. Simulation models should include plant structure and function.’. *Ann. For. Sci.* **57**, 513–520.
- Pagés, L. and J. Kervella: 1990, ‘Growth and development of root systems: geometrical and structural aspects.’. *Acta Biotheoretica* **38**, 289–302.
- Radcliffe, D. E., R. E. Phillips, D. B. Egli, and L. Meckel: 1986, ‘Experimental test of a model of water uptake by soybean.’. *Agron. J.* **78**, 526–530.
- Richards, L. A.: 1931, ‘Capillary conduction of liquids in porous media.’. *Physics* **1**, 318–333.
- Riopell, J. L.: 1969, ‘Regulation of lateral root positions.’. *Bot. Gaz.* **130**, 80–83.
- Rose, D. A.: 1983, ‘The description of the growth of root systems.’. *Plant and Soil* **75**, 405–415.
- Smit, A. L., A. G. Bengough, C. Engels, M. van Noordwijk, S. Pellerin, and S. C. de Geijn: 2000, *Root Methods*. Berlin: Springer.
- Van Genuchten, M. T.: 1980, ‘A closed–form equation for predicting the hydraulic conductivity of unsaturated soils.’. *Soil Sci. Soc. Am. J.* **44**, 892–898.
- Wilderotter, O.: April, 2001, ‘Adaptive Finite-Elemente Methoden für singuläre parabolische Probleme.’. Ph.D. thesis, Universität Bonn, Mathematisch-Naturwissenschaftliche Fakultät.